

Study on the Mass Transfer Enhancement in Biofilms Applied in Papermaking Wastewater Treatment

Mei Pan,^{a,b,c} Jinlong Yan,^{a,c} Cheng Ding,^{a,c,*} Weixing Ma,^{a,c} Jianxiang Jin,^a Ye Yuan,^a and Yuxi Chen^a

The research and refinement of papermaking wastewater treatment and reuse technology are important measures for energy conservation and emission reduction in the papermaking industry. This paper studied the process of biofilm formation and dissolved oxygen mass transfer of biofilms cultivated under different aeration intensities and attempted to enhance the biofilm reactor performance. The removal efficiencies of the chemical oxygen demand, total nitrogen, and ammonia nitrogen through biofilm treatment in two parallel biofilm reactors were higher under the larger aeration intensity (8 L/min) than under the smaller intensity (4 L/min). Macroscopically, this reflected the effect of dissolved oxygen on nitrogen removal. Microscopically, in terms of the dissolved oxygen profiles inside of the biofilms determined using a microelectrode probe, both aerobic and anaerobic layers occurred inside the biofilms, which suggested that simultaneous nitrification and denitrification occurred. The different aeration intensities led to differences in the internal and external dissolved oxygen concentrations in the biofilms, which affected the biofilm growth. This led to different micro-structures, and so the internal metabolism and wastewater treatment performance of the biofilms were not identical.

Keywords: Biofilm; Mass transfer; Dissolved oxygen; Microelectrode

Contact information: a: College of Environmental Science and Engineering, Yancheng Institute of Technology, Yancheng 224003, China; b: College of Environment, Hohai University, Nanjing 210098, P.R. China; c: Key Laboratory for Ecology and Pollution Control of Coastal Wetlands, School of Environmental Science and Engineering, Yancheng Institute of Technology;

* Corresponding author: ycdingc@163.com

INTRODUCTION

Treating papermaking wastewater to reduce the discharge of pollutants in effluent has been thoroughly studied. Biofilms are a commonly used method for this treatment. The mechanism involves microbial communities assembling on a carrier to form biofilms that propagate by adsorbing and decomposing organic matter in wastewater, thus achieving sewage purification (Mašić *et al.* 2010).

In the wastewater treatment process, a biofilm reaction system is usually constructed with a three-phase composition (liquid, gas, and solid) through turbulent fluctuation, in which the mass transfer can be driven to stimulate the degradation reaction of wastewater pollutants. Therefore, the mass transfer is one of the most vital factors in biofilm treatment. One way to enhance oxygen transfer in a biofilm is to directly feed the biofilm gaseous oxygen through aeration (Pan *et al.* 2016; Mendoza-Lera *et al.* 2017), which also accelerates soluble substrates being transferred by diffusion from the liquid (generally aqueous) phase circulated along the inside of the biofilm (Picard *et al.* 2012).

Different aeration intensities (disturbance) might result in different dissolved oxygen (DO) concentrations in the wastewater and inner biofilm, and hence lead to different mass transfer performances inside the biofilm, hydraulic conditions for

biofilm growth, and biofilm thickness and growth states (Visser *et al.* 1996). Additionally, as DO migrates from the biofilm-water interface to the inner biofilm, microbes consume DO, which may also result in different internal biofilm micro-environments.

The purification performance of biofilms, especially the removal of nitrogen, should be examined first from a macroscopic point of view. Nitrogen is mainly present in wastewater in the form of ammonia nitrogen ($\text{NH}_4^+\text{-N}$). When the concentration of DO is high enough, $\text{NH}_4^+\text{-N}$ is first converted to nitrites by nitrification and then to nitrates by nitrifying bacteria. Denitrification reactions are carried out under anoxic or anaerobic conditions; nitrates are converted into nitrogen gas by denitrifying bacteria (Ilies and Mavinic 2001). Additionally, the unique stratification of nitrifying and denitrifying bacteria inside the biofilm, due to the limited mass transfer situation or biological consumption, favors simultaneous nitrification and denitrification reactions (Visser *et al.* 1996). During biofilm treatment, oxygen transfer by diffusion limits the nitrification rate more than in a suspended biomass, where convection is more remarkable (Gapes and Keller 2009; Tang *et al.* 2015). Therefore, research on the internal structure, DO, and mass transfer of the biofilm from a microscopic point of view is important for improving biofilm purification performance.

There has been very little research dealing with the micro-structure or the internal and external mass transfer of biofilms. A microelectrode can be used to measure the biofilm thickness and study the gradient distribution of characteristic parameters along the inside and outside depths of the biofilm (perpendicular to the biofilm surface). This gradient represents the change of characteristic parameters at a certain depth inside the biofilm. Additionally, the distribution of aerobic and anaerobic layers can be analyzed by studying the change of DO concentration inside the biofilm structure by utilizing the microelectrode test, which helps to determine the effects of mass transfer (like oxygen transfer) inside the biofilm on the nitrogen removal from a microscopic point of view (He *et al.* 2016).

In the present work, combining both the macroscopic and microscopic points of view, a multidisciplinary approach was adopted to investigate the effect of the aeration intensity on the biofilm formation, oxygen transfer, and spatial distributions of oxygen inside the biofilm. This study attempted to enhance the mass transfer efficiency inside the biofilm, improve the purification performance of biofilm reactors, determine the appropriate aeration intensity, and optimize the operation parameters in the biofilm treatment process. Moreover, the present study also provided a relevant theoretical basis and optimization recommendations, and promoted the evolution of a better biofilm treatment of papermaking wastewater.

EXPERIMENTAL

Laboratory Biofilm Cultivation

The experimental influent wastewater was obtained from the effluent of an internal circulation anaerobic reactor at a papermaking wastewater treatment station of Jiangsu Huatai Paper Co., Ltd., Yancheng, China. The basic characteristics of the experimental papermaking wastewater are listed in Table 1.

Table 1. Influent Water Quality of the Experimental Reactor

Water Quality Index	pH	COD (mg/L)	TN (mg/L)	$\text{NH}_4^+\text{-N}$ (mg/L)	SS (g/L)
Concentration	7.39	500	14.15	7.05	1.844

COD – chemical oxygen demand; TN – total nitrogen; SS – suspended solids

The experimental setup used in this work involved two sets of parallel operating aeration biofilm reactors that were self-designed. The inoculated sludge was obtained from the activated sludge of a city sewage treatment plant. For each set of experimental devices, there were two peristaltic pumps connecting the reactor and both the influent and effluent containers for adjusting the hydraulic retention time. Different aeration intensities were achieved by using an air pump. Additionally, a motor stirrer was designed in the influent container for preventing natural precipitation and maintaining a homogeneous wastewater quality. A carbon fiber mat was placed in a uniform layer in the reactors to act as the biofilm carrier. The experimental set-up is schematically represented in Fig. 1. The experiment period was 50 d, and the reactors operated for 12 h each day. The process of aeration lasted for 2 h (controlled by the time switch socket) every day with airflows of 8 and 4 L/min. Upon completion of aeration, the overlying water was deposited overnight and measured.

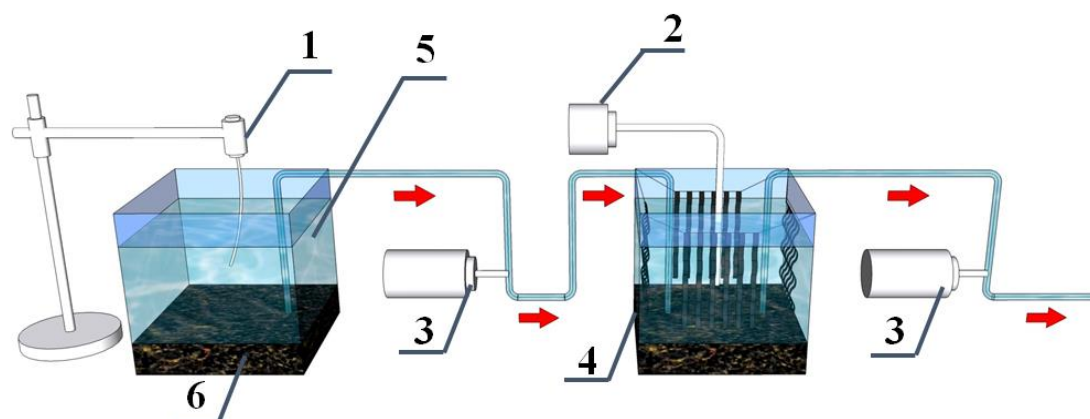


Fig. 1. Schematic diagram of the experimental setup for cultivating the biofilm: 1. motor stirrer; 2. air pump; 3. peristaltic pump; 4. reactor; 5. water; 6. reservoir

Sampling

The sampling dates were the 8th, 15th, and 32nd day for the scanning electron microscopy (SEM) analysis, the 25th, 32nd, and 42nd day for the microelectrode profile analysis, and the 8th, 16th, 22nd, 28th, 35th, 42nd, and 48th day for conventional water quality monitoring.

Analytical Methods

The $\text{NH}_4^+\text{-N}$ content was determined by Nessler's reagent spectrophotometry. The total nitrogen (TN) and nitrate nitrogen ($\text{NO}_3^-\text{-N}$) were detected by ultraviolet spectrophotometry. The calcium ion (Ca^{2+}) concentration was measured experimentally by flame atomic absorption spectrometry. The chemical oxygen demand (COD) was detected by the potassium dichromate oxidation method (State Environmental Protection Administration of China 2002). The pH was measured with a portable dissolved oxygen analyzer (HQ30d, HACH, Shanghai, China).

The DO concentration in the biofilms was measured using a microelectrode profile analysis system, which was also used for assessing the viability and thickness of the biofilms. The system consisted of a 3D microelectrode propeller with a maximum accuracy of 10 μm and an oxygen microelectrode (OX25, Unisense, Århus, Denmark) with a tip diameter of 25 μm and response time of approximately 5 s. The microelectrode was connected to a picoampere meter (MM-Meter, Unisense), and the measuring signals were recorded on a PC with a custom-made data acquisition system. During measurement, the tip of the microelectrode touched the surface of the carbon fiber mat. This measurement was assisted with an electronic digital microscope connected to a computer at 100 \times magnification.

Scanning Electron Microscopy (SEM)

Prior to the SEM observations, biofilm samples were subjected to rigorous processing steps, which included fixation, dehydration, and sputter-coating with gold to ensure a good electrical conductivity. Biofilm samples scraped down from the reactor were placed on glass slides; then they were gradually dehydrated with a series of ascending concentrations (70%) of ethanol (Simões *et al.* 2007), and finally examined with a scanning electron microscope (S-3400N II, Hitachi, Tokyo, Japan). The SEM observations were documented through the acquisition of at least 20 representative micrographs.

RESULTS AND DISCUSSION

Effect of the Aeration Intensity on the Papermaking Wastewater Quality

Effect of the aeration intensity on the removal performance of the chemical oxygen demand

For the two different aeration intensities in the biofilm reactors, the removal performance of the COD is illustrated in Fig. 2. In the early biofilm formation stage, the speed of biological attachment under the larger aeration intensity (8 L/min) was slower than for the smaller intensity (4 L/min), which might have been because the more severe water turbulence under the higher turbulence level obstructed the biofilm forming process (Menniti *et al.* 2009). Nevertheless, the removal efficiency of the COD for the larger aeration intensity was higher because the DO concentration in the wastewater was higher when the aeration was more intense, which accelerated the mineralization of organic pollutants (Mendoza-Lera *et al.* 2017).

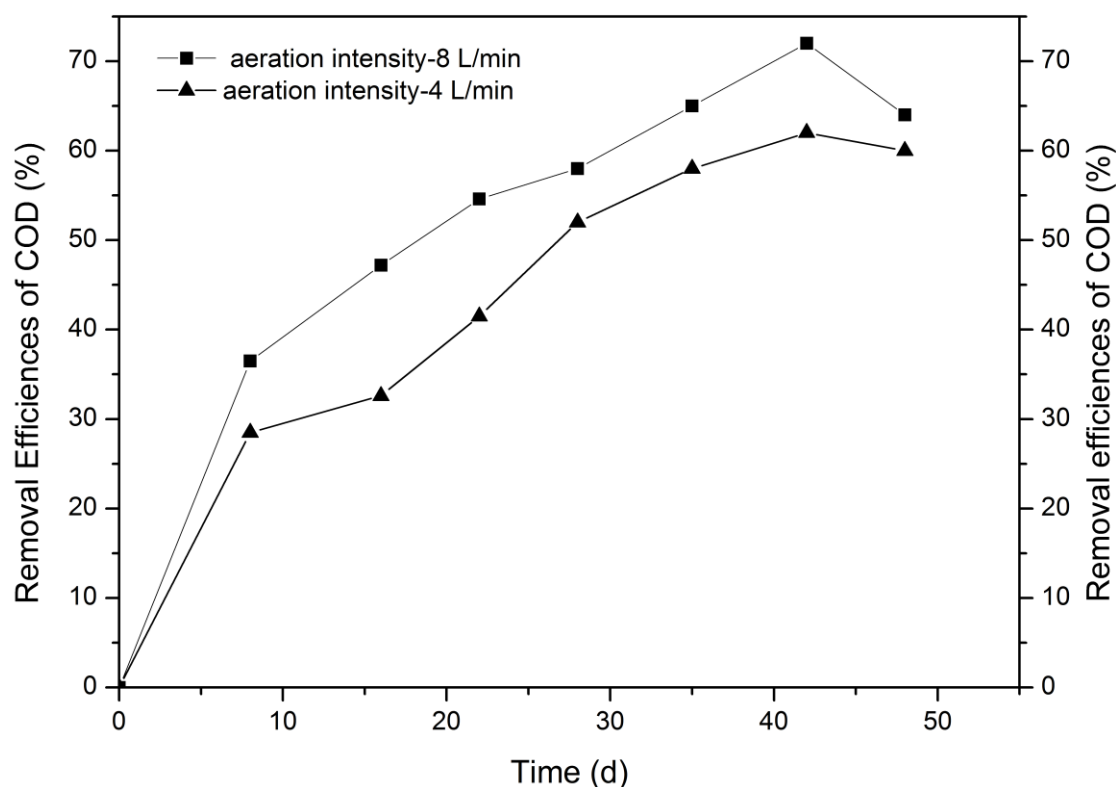


Fig. 2. Removal efficiencies of COD in the effluent

As cultivation continued, the COD removal efficiencies increased to around 90% (maximum) on the 42nd day. This could have been because biofilms had already formed in the early stage of cultivation, and they gradually increased the secretion of extracellular polymeric substances (EPSs) over time. Additionally, the larger aeration intensity increased the turbulence amplitude, which in turn increased the contact opportunity for aquatic organisms and EPSs. Therefore, the much easier biological attachment gave rise to a faster biofilm formation speed (Li *et al.* 2008). It can be said that the removal of organic pollutants is the integrated purification effect of both the aquatic organisms and biofilms with the participation of DO (Mendoza-Lera *et al.* 2017). Purification was dominated by the aquatic organisms in the early stage, but shifted towards being dominated by the biofilms with each successive day, particularly in the middle and late stages. However, the COD removal rate decreased a little after 48 d for both the large and small aeration intensities, which might have been a result of biofilm detachment in the microbial growth cycle (Visser *et al.* 1996).

Effect of the aeration intensity on the removal performance of NH₄⁺ and TN

Figure 3 shows the removal performances of NH₄⁺ and TN under the different aeration intensities. During the experiment, both the NH₄⁺ and TN concentrations underwent noticeable reductions, which suggested the existence of nitrification and denitrification reactions in the biofilm reactors. Especially after 16 d, the removal efficiencies of NH₄⁺ increased to approximately 60% to 85% and reached a maximum of 85% (8 L/min) and 75% (4 L/min) on the 35th day. As cultivation went on, the removal efficiencies of NH₄⁺ first increased and then decreased, which might have been caused by the conversion of organic nitrogen in the activated sludge to NH₄⁺. Meanwhile, for both reactors, the biofilms began to partially fall off after 42 d. However, the removal rate of NH₄⁺ under the higher aeration intensity tended to be higher than under the weak aeration intensity, which was consistent with the experimental conclusions of Nie (2015). Within a certain aeration intensity range, the DO concentration increases with the increasing aeration, and thus improves the activity and metabolism of the nitrite oxidizing bacteria that are aerobic and contribute to the greater removal performance of NH₄⁺ in the treatment of papermaking wastewater (Picard *et al.* 2012). In contrast, if the aeration intensity is small, the low DO concentration will reduce the activity of the nitrite oxidizing bacteria, as well as the removal efficiency of NH₄⁺.

According to Fig. 3, the removal performances of TN under both of the aeration intensities were high. As the experiment continued, the TN removal efficiencies gradually increased, up to 50% to 75% in the middle and late stages, and reached a maximum on the 42nd day (8 L/min: 72%; 4 L/min: 61.2%), which was also in line with the results of Nie (2015). Hence, over a certain aeration intensity range, increasing the aeration results in a higher concentration of DO, which can facilitate not only the microbial metabolism, but also attachment onto the biofilms. A higher microbial attachment can change the biofilm structure and may hinder the oxygen transfer process, which helps to form an anaerobic zone on the biofilm carrier to a certain degree and accelerates the denitrification reaction in the anaerobic layer.

Also, it was obvious that the maximum TN removal occurred approximately a week after the maximum removal of NH₄⁺, which was probably because of the progressive formation of the biofilm anaerobic layer. At the same time, it was inferred that the inoculated sludge that originated from the wastewater treatment plant was beneficial to biofilm formation, and in particular the ammonia-oxidizing, nitrifying, and denitrifying bacteria in the sludge may have greatly promoted the denitrification efficiency of the biofilms (Mußmann *et al.* 2013).

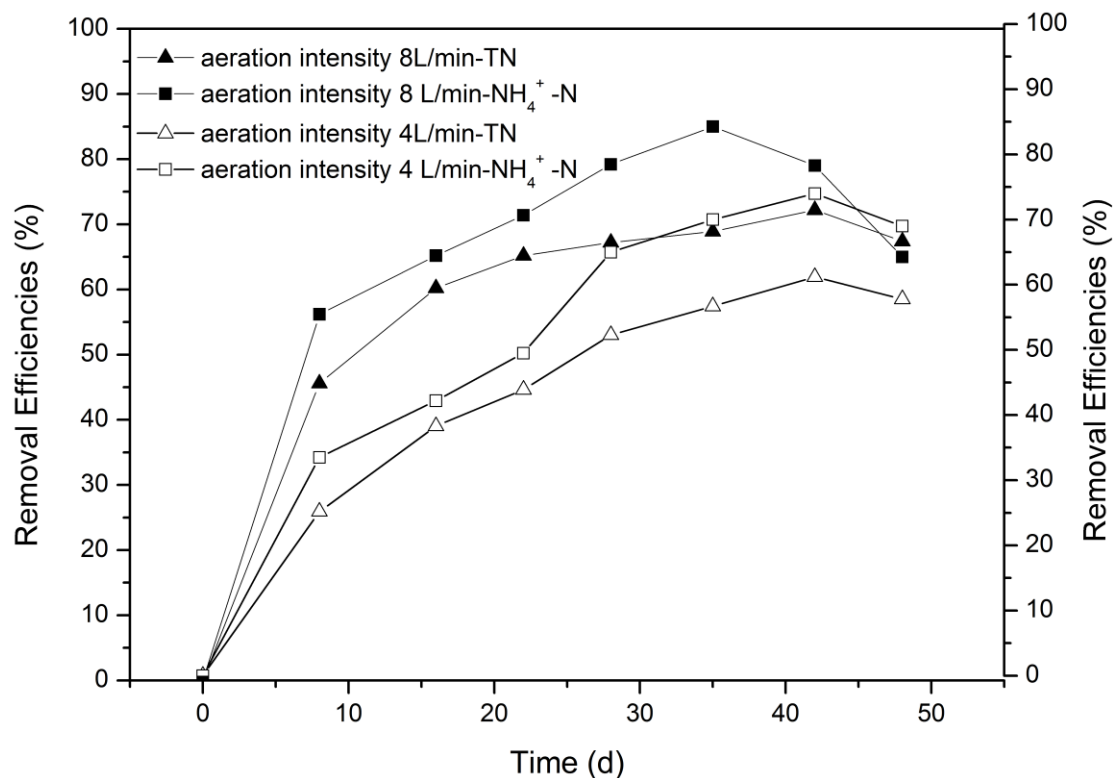


Fig. 3. Removal efficiencies of NH₄⁺-N and TN under different aeration intensities

Effect of the aeration intensity on the removal performance of Ca²⁺

To achieve zero-emissions, it was necessary to carry out a closed recycling of the papermaking wastewater. However, repeated use of wastewater can cause further deterioration of the water quality. The accumulation of Ca²⁺ is a problem because Ca²⁺ reacts with resin acid and SO₄²⁻ to produce CaSO₄, which can form a solid precipitation layer on the forming fabric of paper machines and lead to many problems, such as blocking, fouling, *etc.* (Wäsche *et al.* 2002). Hence, analysis of the removal efficiency of Ca²⁺ under different aeration intensities, as well as the relevant influencing factors, was important for estimating the negative impact of Ca²⁺ on the experiment.

Table 2. Removal Efficiencies of Ca²⁺ under Different Aeration Intensities

	IC Effluent	Aeration Intensity 4 L/min	Aeration Intensity 8 L/min
Ca ²⁺ Concentration (mg/L)	77.2973	28.5405	17.8378
Ca ²⁺ Removal efficiencies (%)		63.08	76.92

As shown in Table 2, despite the high concentration of Ca²⁺ in the papermaking wastewater, the biofilm treatment method demonstrated great removal performances for both the large and small aeration intensities, similar to the results of Huang and Pinder (1995). During the formation process of the biofilms, aggregated microbes generate EPS that has the capability of adsorbing and combining part of Ca²⁺ onto the biofilms, which can help to construct a more stable biofilm structure with a stronger ability of adjusting to the outer environment (Arp *et al.* 2001). The reason why the Ca²⁺ removal efficiency appeared higher under the greater aeration intensity might have been because the microbes on the biofilms produced more EPSs to resist the shear force of the wastewater under the stronger water turbulence (Beyenal and Lewandowski 2002; Leitão *et al.* 2006). More EPSs were able to adsorb

and combine more Ca^{2+} , which greatly relieved the negative influence of Ca^{2+} on the recycling of the papermaking wastewater (Chen *et al.* 2016).

Biofilm Structure

During the colonization period in the experimental simulation systems, biofilms steadily gathered on the carbon fiber mat. The SEM micrographs of the biofilms showed that bacteria and algae were embedded in their self-secreted EPSs, and some voids and channel systems existed in the biofilms (Fig. 4). The voids and channel systems supposedly facilitated the transport of oxygen and nutrients (Hannig *et al.* 2010).

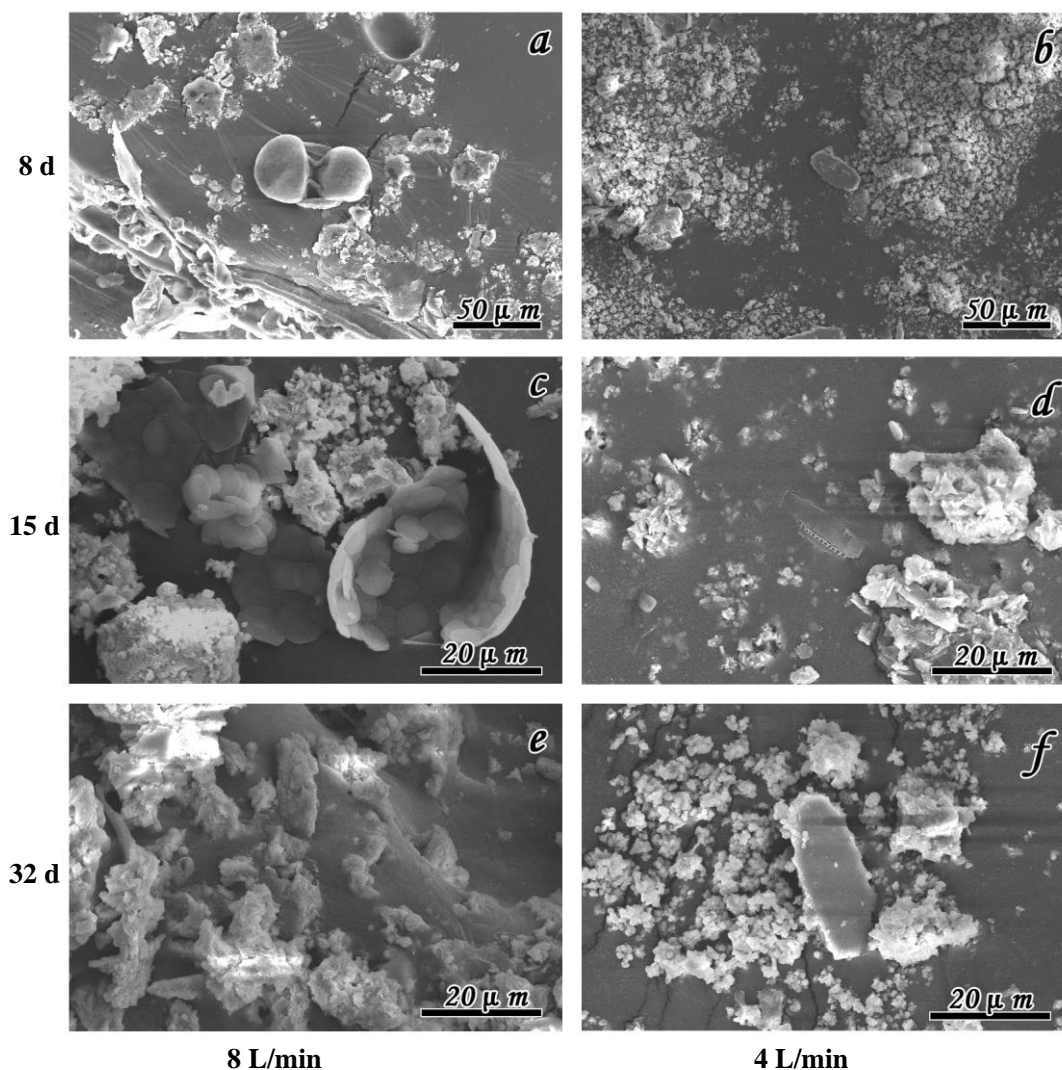


Fig. 4. SEM micrographs of 8- (a, b), 15- (c, d), and 32-d old (e, f) biofilms formed on the carbon-fiber felt under different aeration intensities.

Selected SEM micrographs (Fig. 4) revealed that for the smaller aeration intensity the microbiota that formed and attached to the biofilms were all relatively dispersed and scattered. Most of the microflora were small and not gathered in large groups. In contrast, the microbiota on the biofilms were relatively concentrated under the larger aeration intensity. Although the surface was rough and some irregular protrusions occurred, the biofilm structure was very compact because the bacteria grouped together to form biofilms. Therefore, the amount of biofilms was larger when the aeration intensity was stronger, and the structure might have been more compact as a consequence of the more intense hydraulic scouring (Menniti *et al.* 2009; Graba

et al. 2013). Channel systems in the biofilms growing under the low-intensity aeration could have been extensive, whereas the biofilms growing under the high-intensity aeration were generally more compact with less spacious voids. Although the morphology of the biofilms might have been altered by the dehydration process (Simões *et al.* 2007), the SEM results provided good comparative information that demonstrated clear differences in the structure of the biofilms generated under different aeration conditions. These results also showed that biofilms are in fact highly dynamic. Adaptations can be immediate, allowing the biofilm to change its shape by yielding to the flow and becoming more streamlined (Piqué *et al.* 2016).

Analysis of Oxygen Transfer Inside the Biofilms

The calculation method of the biofilm thickness is presented below. Based on the change in the DO concentrations and auxiliary of the micro-magnifier, the microelectrode probe was moved down slowly through the water to the biofilms under the control of the motor. When the DO level dropped suddenly, it was thought that the probe had entered the biofilm. Because the carbon fiber mat may be attached to the biofilm on both sides, the values measured using the microelectrode probe were symmetrical, so it was difficult for an anaerobic zone to form at the bottom of the biofilm. The oxygen transfer was not limited because of the high porosity of the carbon fiber mat. In contrast, the small number of microbes and lack of aerobic microorganisms did not consume any more DO. Hence, the DO concentration did not decrease, which meant that the microelectrode probe had reached the carbon fiber mat carrier and could help determine the biofilm thickness (Zhou *et al.* 2017).

Oxygen transfer inside the biofilms at different times

Biofilms that were attached to the carbon fiber mat on the 25th and 32nd days under the smaller aeration intensity were chosen for the DO microelectrode measurement. The DO concentration change at different biofilm depths, as well as the biofilm thickness, was measured to analyze the effect of different cultivation times on the mass transfer. The DO profiles inside the biofilms on the 25th and 32nd days during cultivation are illustrated in Figs. 5a and 5b, respectively.

According to the changing trend of the DO concentration in Fig. 5a, the biofilm thickness was determined to be 660 μm . As the biofilm depth increased, the DO concentration gradually decreased from the biofilm-water interface (195 $\mu\text{mol/L}$) to the bottom of the biofilm (135 $\mu\text{mol/L}$), which indicated a mean DO decrease rate of 9.09 $\mu\text{mol}/(\text{L}\cdot 100 \mu\text{m})$. In this zone, the biofilm was looser, and it was easier for oxygen transfer to occur. Additionally, as the microelectrode probe penetrated the entire biofilm, the DO decrease rate inside the biofilm remained constant, despite the increasing biofilm depth, which suggested that the zone inside the biofilm was totally aerobic (Piculell *et al.* 2016).

From Fig. 5b, the biofilm thickness was found to be approximately 800 μm . Similar to the trend in Fig. 5a, the DO concentration gradually decreased from the biofilm-water interface (260 $\mu\text{mol/L}$) to the bottom of the biofilm (145 $\mu\text{mol/L}$), with a mean DO decrease rate of 14.4 $\mu\text{mol}/(\text{L}\cdot 100 \mu\text{m})$. Additionally, the decrease in gradients of the DO differed inside the biofilm, which was consistent with the research hypothesis of Chen (2016). The mean DO decrease rate in the depth range of 420 to 800 μm (20.00 $\mu\text{mol/L}$) was far higher than that in the range of 0 to 420 μm (8.16 $\mu\text{mol/L}$), which implied that the former zone was dominated by aerobic microorganisms because of the larger consumption of DO, and the latter zone might have been an anaerobic layer because of the lower DO consumption.

Moreover, there was a phenomenon where both aerobic and anaerobic zones existed inside the biofilm on the 32nd day. This did not occur in the biofilm on the 25th day, which suggested there was a more suitable environment for simultaneous

nitrification and denitrification favored by both aerobic and anaerobic bacteria in the middle and late stages of the cultivation process. This was also consistent with the results in the *Effect of the aeration intensity on the removal performance of NH_4^+ and TN* section (Ning *et al.* 2014).

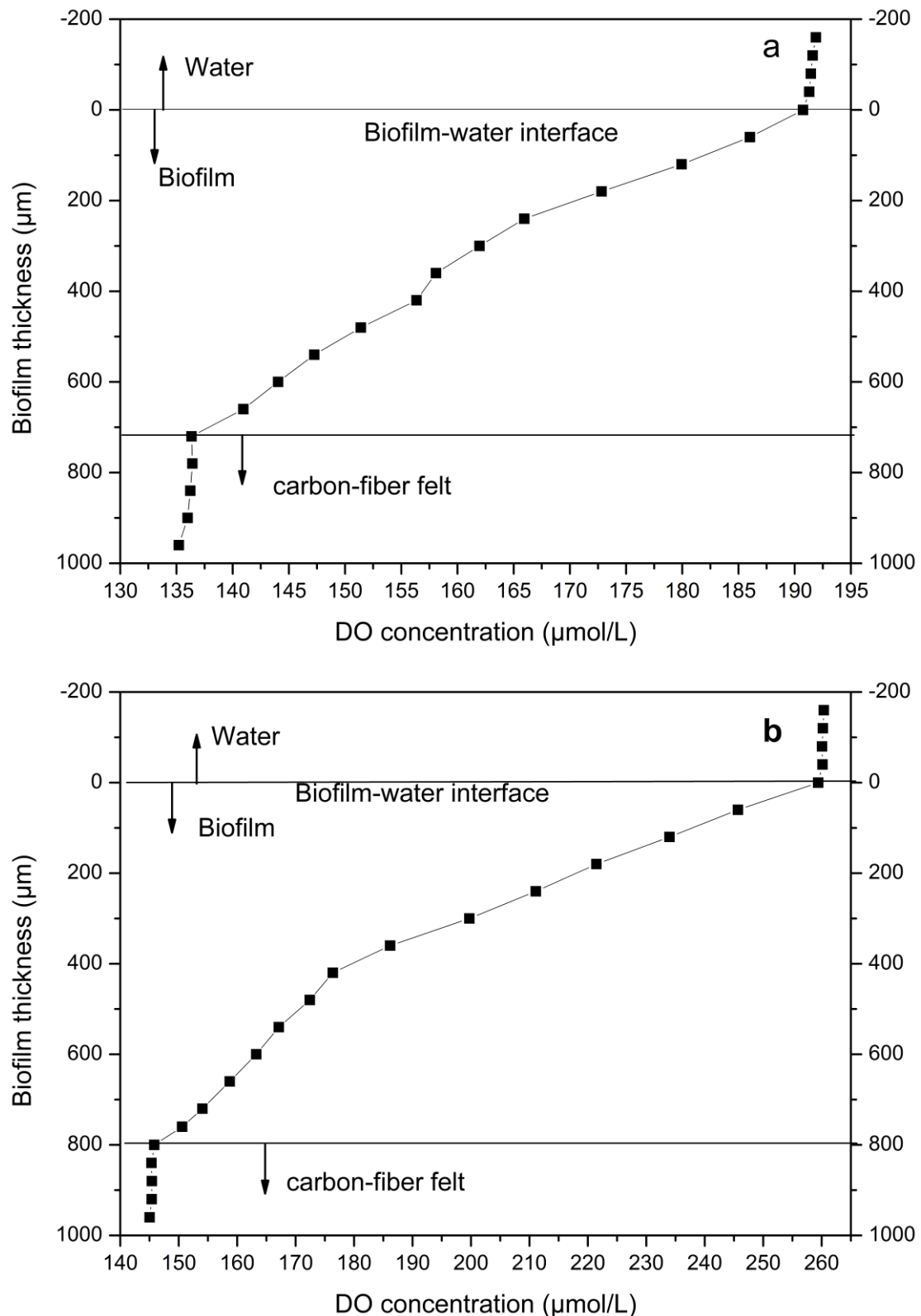


Fig. 5. DO profiles inside the biofilm on the 25th (a) and 32nd days (b) under an aeration intensity of 4 L/min

Oxygen transfer inside the biofilms under different aeration intensities

Biofilms on the carbon fiber mat carrier on the 42nd day for the two different aeration intensities (8 and 4 L/min) were analyzed using the microelectrode profile analysis system. The DO concentrations at various biofilm depths were determined for the DO distribution analysis, and are illustrated in Fig. 6 (Fig. 6a: 8 L/min; Fig. 6b: 4 L/min).

Figure 6a shows that the biofilm thickness was approximately 540 μm . The DO concentration decreased from the biofilm-water interface (280 $\mu\text{mol/L}$) to the bottom of the biofilm (110 $\mu\text{mol/L}$), with a mean DO decrease rate of 31.48 $\mu\text{mol}/(\text{L}\cdot 100\ \mu\text{m})$. Additionally, the mean DO decrease rate per 100 μm within the depth range of 0 to 320 μm (40.93 $\mu\text{mol/L}$) was much higher than that in the range of 320 to 540 μm (18.18 $\mu\text{mol/L}$), which indicated that the former and latter zones were aerobic and anaerobic layers, respectively (Chen 2016).

For the smaller aeration intensity, the biofilm thickness was approximately 660 μm (Fig. 6b). The decrease trend of DO was also in line with Fig. 6a. From the biofilm-water interface to the bottom of the biofilm, the DO concentration decreased from 225 to 101 $\mu\text{mol/L}$, with a mean DO decrease rate per 100 μm of 18.79 $\mu\text{mol/L}$. The mean DO decrease rate for the 0 to 350 μm depth range (26.57 $\mu\text{mol}/(\text{L}\cdot 100\ \mu\text{m})$) was also much larger than that for the 350 to 660 μm range (8.06 $\mu\text{mol}/(\text{L}\cdot 100\ \mu\text{m})$), which indicated that the former and latter zones were aerobic and anaerobic, respectively, similar to the above results.

The stratification of aerobic and anaerobic layers in the biofilm indicated that simultaneous nitrification and denitrification reactions occurred. In the aerobic layer, the DO concentration was relatively higher, which created beneficial conditions for nitrification. However, as a consequence of the large DO consumption by nitrifying bacteria in the aerobic layer, the anaerobic layer lacked DO, which promoted the activity of the denitrifying bacteria, and enhanced the denitrification process. Nevertheless, on the basis of the changing DO decrease rate, it was found that the DO concentration dropped with the increasing depth of the microelectrode probe entering the biofilm, which led to a lower activity of the nitrifying bacteria. This could have been mainly because of the rising consumption of DO limited mass transfer inside the biofilm, and contributed to weakened nitrification and enhanced denitrification.

By comparing the mass transfer inside the biofilm under different aeration intensities, it was obvious that the DO decrease rate in Fig. 6a was higher than that in Fig. 6b, as the biofilm depth increased. Additionally, as shown in Fig. 4, the biofilms grown under the higher aeration intensity were much more compact than under the lower aeration intensity. The biofilm thickness under the stronger hydraulic turbulence appeared smaller, which further confirmed the result that biofilms under the elevated aeration intensity were more compact and thinner.

Figures 5a, 5b, and 6b show that the biofilm thickness and compactness were obviously different during the biofilm formation process under the same aeration intensity (4 L/min), which might have been related to the growth time of the biofilms. The biofilm thickness on the 32nd day was greater than on the 25th and 42nd days. Although the biofilm thickness became greater over time, the DO concentration also decreased as a result of more aerobic microbial consumption. In contrast, the microbes weakly attached to or combined onto the biofilm might have fallen off more easily because of the water turbulence. Moreover, with the formation of the biofilms, the microbial cells generated tightly bound extracellular polymeric substances (TB-EPS) to protect the microbes wrapped up by slime bound extracellular polymeric substances (SB-EPS) and loosely bound extracellular polymeric substances (LB-EPS), which made the biofilms more compact and stable.

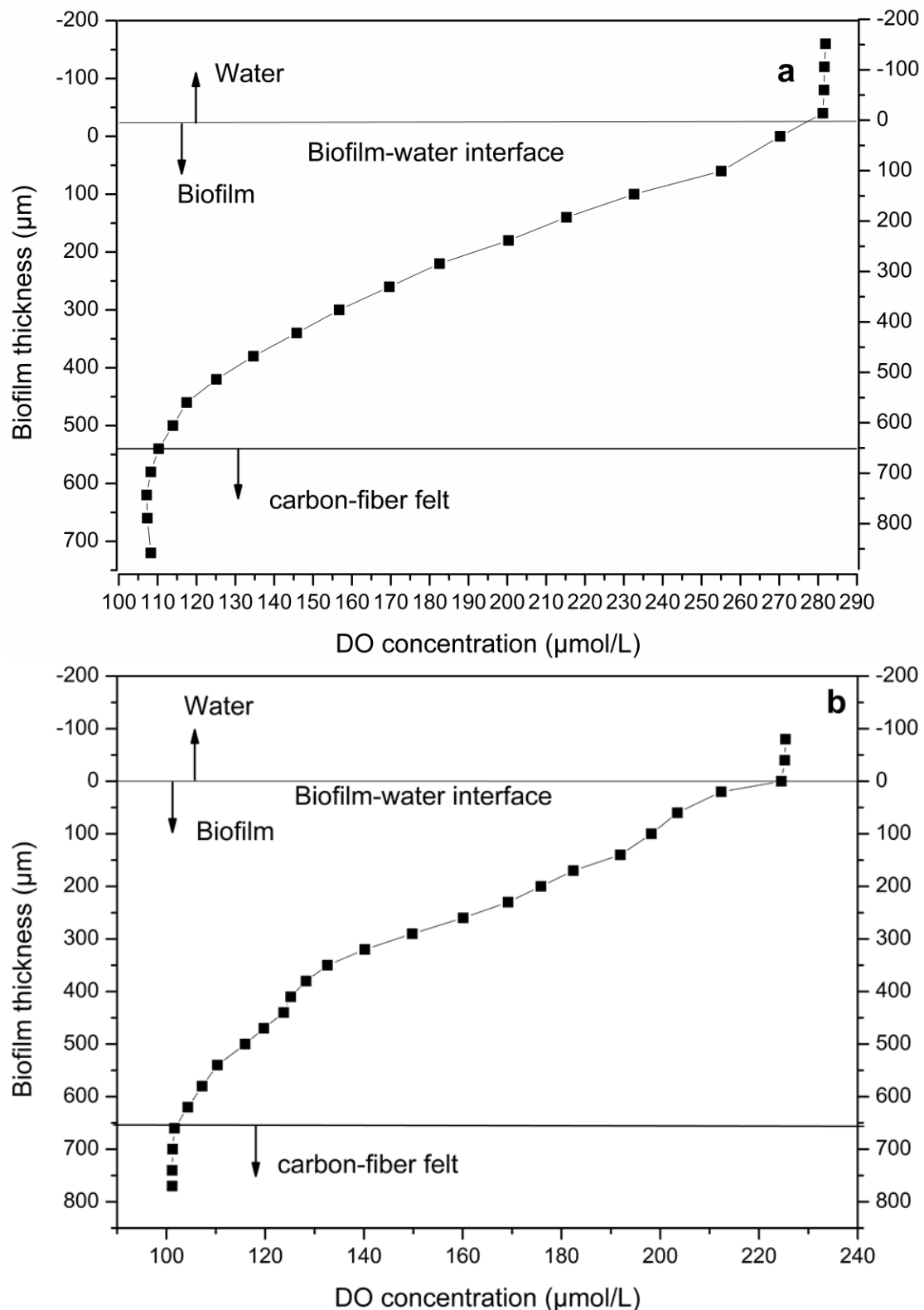


Fig. 6. DO profiles inside the biofilm on the 42th day under an aeration intensity of 8 L/min (a) and 4 L/min (b)

Under the 4 L/min aeration intensity, the DO concentration increased from the 25th (195 μmol/L) to the 32nd day (260 μmol/L), which indicated that, although the organisms in wastewater during the early stage consumed abundant amounts of DO, the supply rate exceeded the consumption rate over time. This in turn improved the DO concentration (Pan *et al.* 2016). However, the DO decreased to 225 μmol/L on the 42nd day, which might have been because of the stronger oxidation reaction of NH_4^+ caused by more aerobic microbes on the biofilms. This was consistent with the results

shown in Fig. 3, where the removal performances of both NH_4^+ and TN were the greatest on the 42nd day.

Though the DO concentration might have differed under different aeration intensities and cultivation times, it decreased to the initial DO level from the biofilm-water interface to the bottom of the biofilm. At the same time, the decrease in the gradient of DO was greater when closer to the biofilm-water interface. This may have been because the DO concentration was affected by the mass transfer resistance inside the biofilm. Also, more aerobic bacteria stayed near the biofilm surface, which led to a greater oxygen consumption in the aerobic reaction (Garny *et al.* 2008; Pan *et al.* 2016). Similarly, the DO decrease gradient was lower near the bottom of the biofilms, probably because of the facultative and anaerobic organisms located there.

Above all, it was concluded that the mean biofilm thickness was affected by the different growth rates of the microbial DO concentration, and ammonium and nitrite transfer. The study further verified the suggestion that this *in situ* measurement system for monitoring the DO distribution in biofilms could be used to determine the mean and maximum thicknesses of the aerobic and anaerobic layers inside of biofilms (He *et al.* 2016).

CONCLUSIONS

1. From a macroscopic perspective, the COD, NH_4^+ , and TN removal efficiencies were high in the two parallel biofilm reactors for both aeration intensities. Their removal efficiencies under the larger aeration intensity (8 L/min) were higher than those under the smaller intensity (4 L/min). Additionally, the adsorption and combination of Ca^{2+} by the EPS generated by the biofilm reduced the negative effect of Ca^{2+} on the recycling of papermaking wastewater.
2. SEM micrographs showed that both the aeration intensity and cultivation time influenced the biofilm growth, including the thickness and compaction. In terms of the DO profiles inside the biofilms, which were analyzed using a microelectrode probe, both aerobic and anaerobic layers occurred inside the biofilms. This suggested that simultaneous nitrification and denitrification occurred. These structural features have important implications for the growth and metabolism of cells in the biofilm by regulating both mass transfer into the biofilm and spatial distribution of oxygen and nutrients inside the biofilm. Ultimately, this coupling between the physical structure and mass transfer induced biogeochemical gradients in the biofilms, which determined the wastewater treatment performance of the biofilms.

ACKNOWLEDGEMENTS

The authors appreciate the support of the National Natural Science Foundation of China (Grant No. 21677119 and 51608467) and the industry-university-research institute cooperation project of Jiangsu Province (No. BY2016065-61). The authors also thank Meili Zhang for her helpful suggestions and corrections on the earlier draft of this study, which were used to improve the content.

REFERENCES CITED

- Arp, G., Reimer, A., and Reitner, J. (2001). "Photosynthesis-induced biofilm calcification and calcium concentrations in Phanerozoic oceans," *Science* 292(5522), 1701-1704. DOI: 10.1126/science.1057204
- Beyenal, H., and Lewandowski, Z. (2002). "Internal and external mass transfer in biofilms grown at various flow velocities," *Biotechnol. Progr.* 18(1), 55-61. DOI: 10.1021/bp010129s
- Chen, C., Xu, H., Su, W.-p., and Dai, H.-q. (2016). "Forming process and mechanism of interferent from DCS and calcium ions in wet end system of paper machine," *Transactions of China Pulp and Paper* 31(2), 11-17.
- Chen, M. (2016). *Effects of Microenvironment on N₂O Produced in Biological Aerated Filter (BAF) Based on Microelectrode Technique*, Master's Thesis, Chongqing University, Chongqing, China.
- Gapes, D. J., and Keller, J. (2009). "Impact of oxygen mass transfer on nitrification reactions in suspended carrier reactor biofilms," *Process Biochem.* 44(1), 43-53. DOI: 10.1016/j.procbio.2008.09.004
- Garny, K., Horn, H., and Neu, T. R. (2008). "Interaction between biofilm development, structure and detachment in rotating annular reactors," *Bioprocess and Biosystems Engineering* 31(6), 619-629. DOI: 10.1007/s00449-008-0212-x
- Graba, M., Sauvage, S., Moulin, F. Y., Urrea, G., Sabater, S., and Sanchez-Pérez, J. M. (2013). "Interaction between local hydrodynamics and algal community in epilithic biofilm," *Water Res.* 47(7), 2153-2163. DOI: 10.1016/j.watres.2013.01.011
- Hannig, C., Follo, M., Hellwig, E., and Al-Ahmad, A. (2010). "Visualization of adherent micro-organisms using different techniques," *J. Med. Microbiol.* 59(1), 1-7. DOI: 10.1099/jmm.0.015420-0
- He, Q., Liu, T., Fan, L., Mei, H., and Ai, H. (2016). "Oxygen distribution of biofilm in biological aerated filter based on microelectrode," *Chinese Journal of Environmental Engineering* 10(9), 4679-4683. DOI: 10.12030/j.cjee.201504051
- Huang, J., and Pinder, K. L. (1995). "Effects of calcium on development of anaerobic acidogenic biofilms," *Biotechnol. Bioeng.* 45(3), 212-218. DOI: 10.1002/bit.260450305
- Ilies, P., and Mavinic, D. S. (2001). "The effect of decreased ambient temperature on the biological nitrification and denitrification of a high ammonia landfill leachate," *Water Res.* 35(8), 2065-2072. DOI: 10.1016/S0043-1354(00)00477-2
- Leitão, R. C., van Haandel, A. C., Zeeman, G., and Lettinga, G. (2006). "The effects of operational and environmental variations on anaerobic wastewater treatment systems: A review," *Bioresour. Technol.* 97(9), 1105-1118. DOI: 10.1016/j.biortech.2004.12.007
- Li, T., Bai, R., and Liu, J. (2008). "Distribution and composition of extracellular polymeric substances in membrane-aerated biofilm," *J. Biotechnol.* 135(1), 52-57. DOI: 10.1016/j.jbiotec.2008.02.011
- Mašić, A., Bengtsson, J., and Christensson, M. (2010). "Measuring and modeling the oxygen profile in a nitrifying moving bed biofilm reactor," *Math. Biosci.* 227(1), 1-11. DOI: 10.1016/j.mbs.2010.05.004
- Mendoza-Lera, C., Frossard, A., Knie, M., Federlein, L. L., Gessner, M. O., and Mutz, M. (2017). "Importance of advective mass transfer and sediment surface area for streambed microbial communities," *Freshwater Biol.* 62(1), 133-145. DOI: 10.1111/fwb.12856
- Menniti, A., Kang, S., Elimelech, M., and Morgenroth, E. (2009). "Influence of shear on the production of extracellular polymeric substances in membrane bioreactors," *Water Res.* 43(17), 4305-4315. DOI: 10.1016/j.watres.2009.06.052

- Mußmann, M., Ribot, M., von Schiller, D., Merbt, S. N., Augspurger, C., Karwautz, C., Winkel, M., Battin, T. J., Martí, E., and Daims, H. (2013). "Colonization of freshwater biofilms by nitrifying bacteria from activated sludge," *FEMS Microbiol. Ecol.* 85(1), 104-115. DOI: 10.1111/1574-6941.12103
- Nie, Y. H. (2015). *Study on the Decontamination Performance of Nitrogen in Polluted Water by Micro-Aeration Enhanced Ecological Floating Bed*, Master's Thesis, Southwest Jiaotong University, Chengdu, China.
- Ning, Y.-F., Chen, Y.-P., Shen, Y., Zeng, N., Liu, S.-Y., Guo, J.-S., and Fang, F. (2014). "A new approach for estimating aerobic-anaerobic biofilm structure in wastewater treatment via dissolved oxygen microdistribution," *Chem. Eng. J.* 255, 171-177. DOI: 10.1016/j.cej.2014.06.042
- Pan, M., Zhao, J., Zhen, S., Heng, S., and Wu, J. (2016). "Effects of the combination of aeration and biofilm technology on transformation of nitrogen in black-odor river," *Water Sci. Technol.* 74(3), 655-662. DOI: 10.2166/wst.2016.212
- Picard, C., Logette, S., Schrotter, J. C., Aimar, P., and Remigy, J. C. (2012). "Mass transfer in a membrane aerated biofilm," *Water Res.* 46(15), 4761-4769. DOI: 10.1016/j.watres.2012.05.056
- Piculell, M., Welander, P., Jönsson, K., and Welander, T. (2016). "Evaluating the effect of biofilm thickness on nitrification in moving bed biofilm reactors," *Environ. Technol.* 37(6), 732-743. DOI: 10.1080/09593330.2015.1080308
- Piqué, G., Vericat, D., Sabater, S., and Batalla, R. J. (2016). "Effects of biofilm on river-bed scour," *Sci. Total Environ.* 572, 1033-1046. DOI: 10.1016/j.scitotenv.2016.08.009
- Simões, M., Pereira, M. O., Sillankorva, S., Azeredo, J., and Vieira, M. J. (2007). "The effect of hydrodynamic conditions on the phenotype of *Pseudomonas fluorescens* biofilms," *Biofouling* 23(4), 249-258. DOI: 10.1080/08927010701368476
- State Environmental Protection Administration of China (2002). *Monitor and Analysis Method of Water and Wastewater*, Chinese Environmental Science Publication House, Beijing, China.
- Tang, B., Qiu, B., Huang, S., Yang, K., Bin, L., Fu, F., and Yang, H. (2015). "Distribution and mass transfer of dissolved oxygen in a multi-habitat membrane bioreactor," *Bioresour. Technol.* 182, 323-328. DOI: 10.1016/j.biortech.2015.02.028
- Visser, P., Ibelings, B. A. S., van der Veer, B., Koedood, J., and Mur, R. (1996). "Artificial mixing prevents nuisance blooms of the cyanobacterium *Microcystis* in Lake Nieuwe Meer, the Netherlands," *Freshwater Biol.* 36(2), 435-450. DOI: 10.1046/j.1365-2427.1996.00093.x
- Wäsche, S., Horn, H., and Hempel, D. C. (2002). "Influence of growth conditions on biofilm development and mass transfer at the bulk/biofilm interface," *Water Res.* 36(19), 4775-4784. DOI: 10.1016/S0043-1354(02)00215-4
- Zhou, X., Sun, Y., Shi, N., and Tian, Y. (2017). "Spatial distribution characteristics of extracellular polymeric substances in a denitrification biological filter," *Chinese Journal of Environmental Engineering* 11(5), 2836-2844. DOI: 10.12030/j.cjee.201512172

Article submitted: September 5, 2017; Peer review completed: November 5, 2017;

Revised version received: November 10, 2017; Accepted: November 12, 2017;

Published: November 19, 2017.

DOI: 10.15376/biores.13.1.299-312